

Article

# Effect of Rheological Properties of Aqueous Solution of Na-CMC on Spray Angle for Conical Pressure-Swirl Atomizers

Krystian Czernek <sup>1,\*</sup>, Marek Ochowiak <sup>2</sup> and Sylwia Włodarczak <sup>2</sup> 

<sup>1</sup> Department of Process and Environmental Engineering, Faculty of Mechanical Engineering, Opole University of Technology, ul. Prószkowska 76, 45-758 Opole, Poland

<sup>2</sup> Department of Chemical Engineering and Equipment, Poznan University of Technology, 60-965 Poznan, Poland; marek.ochowiak@put.poznan.pl (M.O.); sylwia.wlodarczak@put.poznan.pl (S.W.)

\* Correspondence: k.czernek@po.edu.pl; Tel.: +48-77-449-8778

Received: 11 November 2020; Accepted: 26 November 2020; Published: 30 November 2020



**Abstract:** Aerosol is a multiphase system, created as a result of the dispersion of a liquid in a gaseous medium. The atomized liquids are most often water and fuel; however, they can be any other substance. Even a small addition of a substance that changes the rheological properties (i.e., the nature of the flow) can change the properties of the resulting aerosol. The most important parameters that characterize the aerosol are the outflow rate, the droplet diameter, the spray spectrum, and the spray angle. The latter is important when selecting atomizers, especially those working in groups on the sprayer boom. The spray angle is an important parameter of the atomization process, providing a great deal of information about the quality of the spray. This study presents the results of rheological tests and the atomization of aqueous solutions with varying concentrations of sodium carboxymethylcellulose (Na-CMC). We found that the spray angle decreased with increasing Na-CMC concentration in the solution, which is attributable to an increase in shear viscosity. The design of the atomizer is also important. The largest spray angles were obtained for an atomizer with a diameter of 0.02 m and with the inlet port being placed at an angle to the atomizer axis. Based on the experimental results for various liquids and atomizer designs, a correlation equation describing the spray angle is proposed.

**Keywords:** atomization; spray angle; construction of atomizer; sodium carboxymethylcellulose; rheology

## 1. Introduction

Aerosol is a multiphase system, created as a result of the dispersion of a liquid in a gaseous medium. The production of aerosols is extremely important in the engineering, pharmaceutical, and agricultural industries. In order to improve the effectiveness of operation, various types of polymer additives are introduced into the liquid—for example, herbicides in the case of agriculture [1]. Even a small addition can change the rheological properties of the liquid, which also affects the spray angle value, among other things. The addition of a polymer may affect the length of the compact sprayed liquid stream. In the case of atomizing liquids, the increase in the viscosity of polymer solutions inhibits the process of breaking the stream and changes the distribution of the diameters of the droplets formed. The impact of different polymer additions, including sodium carboxymethylcellulose (Na-CMC), on the atomization process was analyzed by Ochowiak and Broniarz-Press [2]. On the basis of the obtained experimental results, they observed that the addition of a polymer caused an increase in the viscosity of the liquid, which in turn resulted in a noticeable change in the length of the compact liquid

stream and limited the process of breaking the stream. Aqueous solutions of polymers are also used as substitutes for oils in the processes of hardening carburized elements.

The spray angle is an important performance parameter in pressure-swirl atomizers. It is defined as the apex angle of the aerosol formed between two straight lines along the jet flowing out of the atomizer. The compact liquid stream becomes narrower as the distance from the atomizer orifice increases. The constriction of the jet is mainly due to the action of the surrounding gas, which is set in motion by the suction action of the liquid jet and the force of gravity. The spray angle can only be clearly measured in a vacuum. This parameter determines the total coverage of the surface with the aerosol, the degree of mixing of the atomized liquid with the surrounding gas, and the degree of dispersion of the liquid stream [3,4]. Knowledge of the spray angle is important in determining the spray area that can be obtained for the atomizer used, which in turn informs the number of atomizers and their location [5]. The optimal spray angle allows for a stable combustion process in gasoline engines with direct injection and, in gas turbines, allows for good ignition performance and helps to reduce the smoke/flame and pollutant emissions [6–9].

That the available literature reports that the spray angle is influenced by the geometry of the atomizer, as well as the properties of the liquid and the density of the medium in which it is atomized [4,5,8,10–14]. The most important geometric parameters include the diameter of the inlet and the orifice, the diameter of the swirl chamber, the length-to-diameter ratio of the orifice, and the height-to-diameter ratio of the swirl chamber [5,14]. Modification of the orifice is also important (e.g., using arcs or slants) [15–19]. The dynamic viscosity of the liquid is of great importance for the spray angle. This parameter has been analyzed by many scientists [9–11]. On the basis of these studies, it was demonstrated that the spray angle decreases with increasing dynamic viscosity of the liquid, as the stream is more difficult to break up and is less aerated.

Lee et al. [4] studied the dependence of the spray angle on the Reynolds number for diesel fuel and Bunker-A fuel. For diesel fuel, it was observed that under stable operating conditions, an increase in the Reynolds number above  $Re_L = 3450$  caused an increase in the spray angle from  $45^\circ$  to  $60^\circ$ , and the differences between the minimum and maximum values were marginal. For the Bunker-A fuel, at a low  $Re_L$  value (around 1500), the spray angle value was minimal, as there was practically no swirling motion. At a Reynolds number value of about  $Re_L = 1650$ , a sudden increase in the spray angle was observed and its value fluctuated. The spray angle value stabilized only at an  $Re_L$  value of around 3300.

Mun et al. [20] studied the spray angle for aqueous solutions of sodium carboxymethylcellulose, using an agricultural swirl atomizer. It was observed that the spray angle initially increased with the increase in the Na-CMC concentration. With a further increase in polymer concentration, the spray angle decreased until the collapse of the cone and an outflow of a single stream occurred. The spray angle behavior can be explained by the different values of extensional viscosity for different types of polymers and their concentrations in aqueous solution. The spray angle for each atomizer slightly increases as the Reynolds number increases to a certain range of its value, after which it causes an increase in the mean tangential velocity to a greater degree than for the mean axial velocity. Once a certain Reynolds number is exceeded for a specific atomizer, the ratio of the mean tangential velocity to the axial velocity at each cross section remains substantially unchanged as the Reynolds number increases further. Increasing the tangential area of the atomizer inlet and the kinematic viscosity of the liquid reduces the spray angle.

Wójtowicz and Kotowski [21] studied conical swirl regulators with different geometries. Regulators are flow devices with a structure similar to atomizers. In their study, the value of the spray angle was analyzed. Based on the research results, a correlation equation describing the tangent of the spray half angle was proposed:

$$\operatorname{tg} \frac{\theta}{2} = 2.8K^{1.61} (\cos(90^\circ - \varphi))^{-1.36} \left( \frac{d_0}{d_p} \right)^{5.2} \left( \frac{H_S}{d_p} \right)^{-0.077} \left( \frac{D_S}{d_p} \right)^{-1.82} \quad (1)$$

where  $K$  is the geometric constant described by Equation (2),  $\phi$  is the tilt angle of the inlet port,  $d_0$  is the diameter of the orifice,  $d_p$  is the diameter of the inlet,  $H_S$  is the height of the swirl chamber, and  $D_S$  is the diameter of the swirl chamber.

$$K = \frac{2R_0(\cos(90^\circ - \phi))r_p^2}{r_0^3} = \frac{2R_0(\cos(90^\circ - \phi))d_p^2}{d_0^3} \quad (2)$$

where  $R_0$  is the radius of the liquid swirl at the inlet,  $R$  is the radius of the swirl chamber, and  $r_0$  is the radius of the inlet port.

The aim of this study was to determine the effect of the concentration (viscosity) of aqueous solutions of sodium carboxymethylcellulose and the construction of modified swirl atomizers on the spray angle value. The impact of dimensions of the swirl chamber (diameter and height) and the position of the inlet port on the jet breakup of the model polymer solution was analyzed.

## 2. Materials and Methods

The most important elements of the experimental setup for atomizing liquids were: pressure-swirl atomizers of various designs, Krohne Messtechnik VA 40 liquid rotameters with measuring ranges of 0.5–5, 4–40, 25–250, and 100–1000 dm<sup>3</sup>/h, an organic glass tank filled with liquid and equipped with a CHI 2-30 pump by Grunfos Poland, a coil, a Center 309 digital thermometer by Center, a Canon EOS-1D Mark III camera with a strobe lamp, and a computer. A simplified diagram of the experimental setup is shown in Figure 1. Due to the lack of adaptation of the rotameters used to measure the flow rate of liquids other than water, it was necessary to scale them each time. This consisted of measuring the weight of the flowing liquid over a specific period of time. For this purpose, a WLC 10/A2 electronic scale from Radwag with an accuracy of 0.1 g was used. The flow rate of the liquid was regulated with poppet valves from Italinox. The flow rate range was from 0 to 250 dm<sup>3</sup>/h. The tests were carried out at a liquid temperature of  $293 \pm 1$  K.

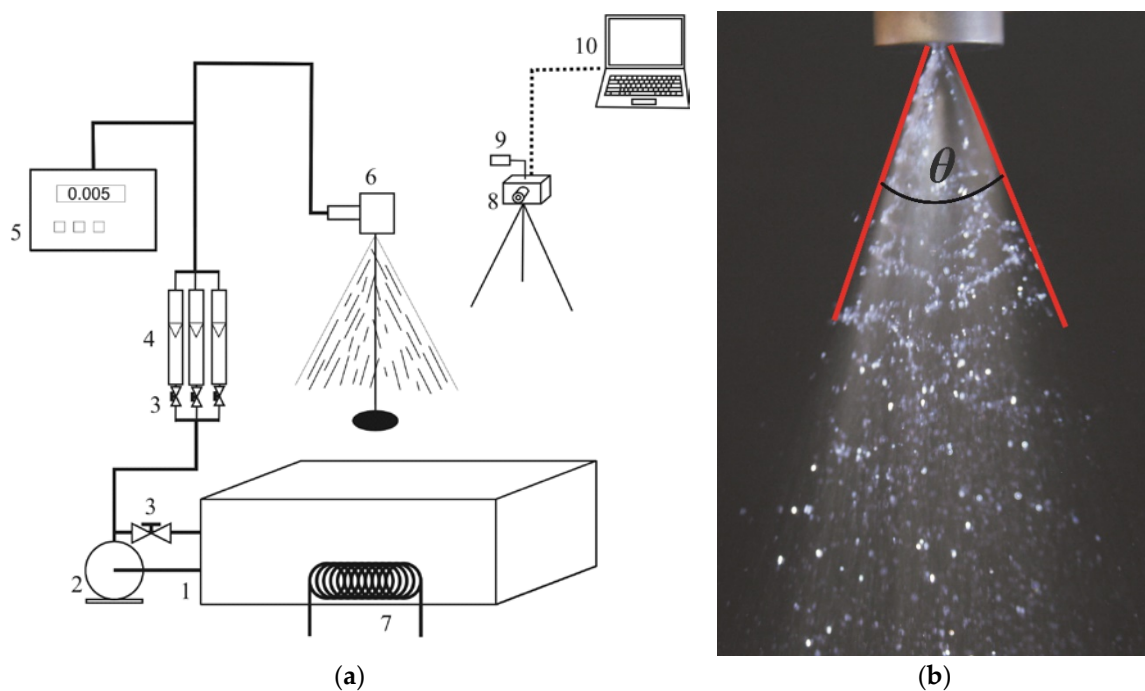


**Figure 1.** Experimental setup and methodology: (a) simplified diagram of the experimental setup: 1—tank, 2—pump, 3—valves, 4—liquid rotameters, 5—pressure gauge, 6—pressure-swirl atomizer, 7—coil, 8—camera, 9—strobe, 10—computer; (b) exemplary photo with the spray angle measured.

The test used pressure-swirl atomizers with the following designs:

- Atomizers with a conical swirl chamber with different height-to-diameter ratios, with an inlet port located perpendicular to the atomizer axis and cylindrical orifices (RSP1, RSP2, RSP3, and RSP4);
- Atomizers with a conical swirl chamber with different height-to-diameter ratios, with an inlet port located at an angle of  $60^\circ$  in relation to the atomizer axis and cylindrical orifices (RSK1, RSK2, RSK3, RSK4, RSK5, RSK6, RSK7, and RSK8).

The diameter of the inlet port in each case was  $d_p = 0.0025$  m. The atomizers are shown in Figure 2. The most important geometric values of these atomizers are shown in Table 1. The dimensional tolerance for the diameter and length of the orifice was  $\pm 50$   $\mu\text{m}$ , while for the diameter and height of the swirl chamber it was  $\pm 100$   $\mu\text{m}$ .

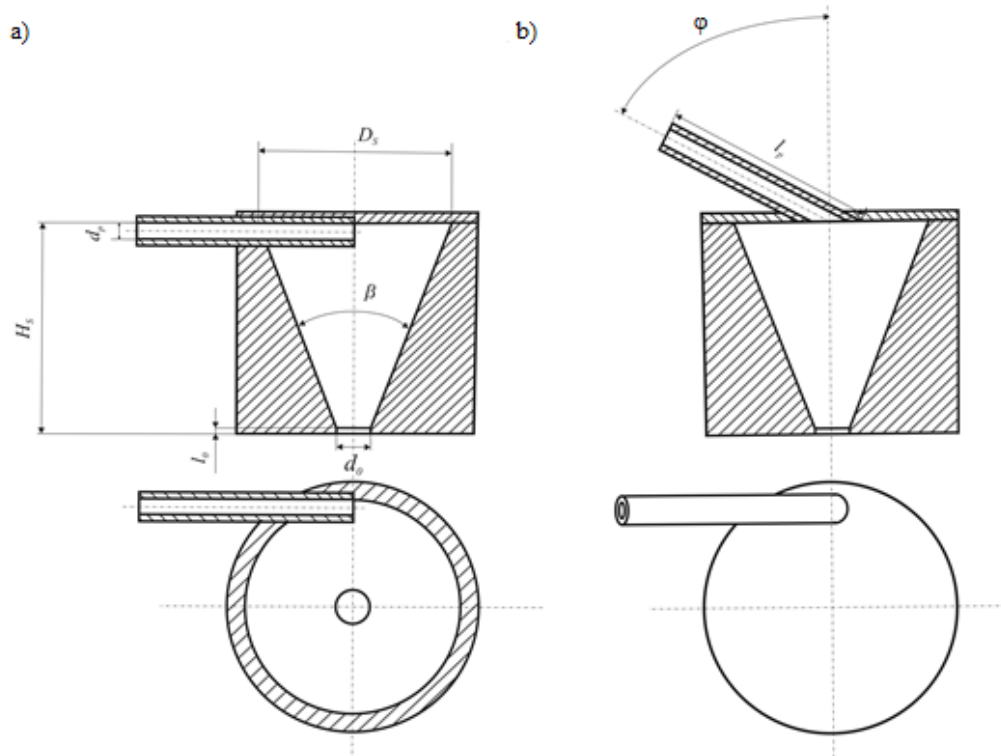


**Figure 2.** Design of pressure-swirl atomizers with a conical swirl chamber: (a) with the liquid fed through the inlet port (RSP) perpendicular to the atomizer axis, and (b) with the liquid fed through the inlet port at an angle  $\phi = 60^\circ$  to the atomizer axis (RSK).

**Table 1.** Geometric dimensions of the tested atomizers with a conical swirl chamber.

Atomizer	$D_s$ (m)	$H_s$ (m)	$d_0$ (m)	$l_0$ (m)	$l_0/d_0$
RSP1	0.020	0.015	0.0025	0.00125	0.5
RSP2	0.020	0.020	0.0025	0.00125	0.5
RSP3	0.020	0.025	0.0025	0.00125	0.5
RSP4	0.020	0.020	0.0025	0.00250	1.0
RSK1	0.020	0.015	0.0025	0.00125	0.5
RSK2	0.020	0.020	0.0025	0.00125	0.5
RSK3	0.020	0.025	0.0025	0.00125	0.5
RSK4	0.020	0.020	0.0025	0.00250	1.0
RSK5	0.040	0.015	0.0025	0.00125	0.5
RSK6	0.040	0.020	0.0025	0.00125	0.5
RSK7	0.040	0.025	0.0025	0.00125	0.5
RSK8	0.040	0.020	0.0025	0.00250	1.0

In order to determine the spray angle, the standard lens setting was used. The photos were taken against a black background in order to obtain the clearest possible contour of the stream. The ISO sensitivity was set to 1000 at a shutter speed of 1/10 s. The Image-Pro Plus software from Media Cybernetics was used for the spray angle analysis. In order to determine the spray angle, after loading a given photo into the program, the spray angle as the measured value had to be selected first, and then two lines limiting the atomized liquid stream had to be drawn. The program automatically gave the value of the spray angle. The accuracy of the spray angle measurement was  $\pm 4^\circ$ .

To measure the shear viscosity, a Physica MCR 501 rotary rheometer from Anton Paar was used. The test used a cone–plate system of CP60-1-SN21572 type with a slit ( $d = 121 \mu\text{m}$ ) in the shear rate range from 51 to 1019 1/s. A Peltier system was used to stabilize the temperature with an accuracy of  $\pm 0.01^\circ\text{C}$ . A K9 tensiometer from Krüss GmbH in the surface tensions measurements was used. The du Noüy method was used.

The test polymer was sodium carboxymethylcellulose (Na-CMC) with a molecular weight of 700,000 and a degree of substitution DS = 0.90, manufactured by Sigma-Aldrich. The physicochemical properties of the tested liquids are summarized in Table 2.

**Table 2.** Properties of tested solutions.

Test Solution	Density $\rho_L$ (kg/m <sup>3</sup> )	Surface Tension $\sigma$ (mN/m)	Characteristic Flow Index $n$ (-)	Coefficient of Consistency $k$ (Pa·s <sup><math>n</math></sup> )
0.1% aqueous Na-CMC solution	999.6	71.5	0.93	0.007
0.2% aqueous Na-CMC solution	999.8	70.9	0.94	0.010
0.3% aqueous Na-CMC solution	999.8	70.6	0.89	0.023
0.4% aqueous Na-CMC solution	999.8	69.9	0.82	0.053

### 3. Results

#### 3.1. Rheological Properties of Tested Liquids

In the case of non-Newtonian fluids, the simplest mathematical rheological model is the Ostwald–de Waele power model with the form:

$$\tau = k \cdot \dot{\gamma}^n \quad (3)$$

where  $\tau$  is the shear stress,  $\dot{\gamma}$  is the shear rate,  $k$  is the consistency coefficient, and  $n$  is the characteristic flow index.

Figure 3 shows the dependence of shear viscosity in the aqueous solutions of sodium carboxymethylcellulose, which showed the characteristics of non-Newtonian fluids. The dynamic viscosity decreased with increasing shear rate in the tested range. The shear viscosity increased with increasing polymer concentration in the solution. The effect of the Na-CMC concentration at low values of  $\dot{\gamma}$  was more pronounced than at high values of  $\dot{\gamma}$  [22]. This may be explained by the fact that a higher concentration of Na-CMC increases the number of polymer chains per unit volume, thereby shortening the distance between polymer chains and enhancing the strength of intermolecular entanglement [23]. If the shear rate applied is small, the network between the chains is relatively stable and is difficult to destroy. If the shear rate applied is high, the convoluted Na-CMC chains are stretched, and the entangled chains' structure can easily be broken as described by Chen et al. [24].

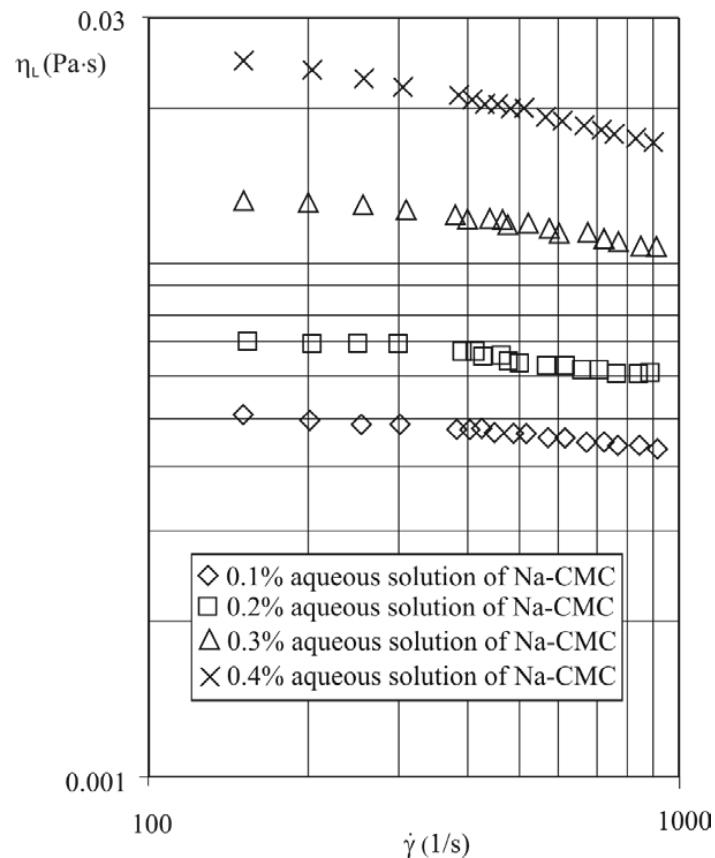


**Figure 3.** Dependence of shear viscosity on shear rate for aqueous solutions of sodium carboxymethylcellulose (Na-CMC).

### 3.2. Spray Angle

Gravity plays practically no important role in the case of pressure-swirl atomizers. From the point of view of the atomizing process, this means that no matter which direction the atomizer is directed (upwards, downwards, or sideways) the resulting spray should always be the same, regardless of the position of the atomizer. At high rotational velocities, on the inner walls of the vortex chamber, we obtained a thin liquid film with a thickness of  $s$ , surrounding the air core. The outside air was sucked in due to the pressure gradient. Since there was no stabilizing force, the air was sucked into the swirl chamber. This effect, which is called an air core, begins when the free surface changes. The diameter of the air core is smaller than the diameter of the atomizer orifice. The air core primarily affects the actual orifice cross section occupied by the liquid, which is less than:

$$A_0 < \frac{\pi d_0^2}{4} \quad (4)$$

The formation of the air core in connection with the spray angle, droplet diameter, and the flow velocity of the liquid in the spray was described by Durina et al. [25]. In a conical swirl chamber (Figure 4), a liquid flows to the atomizer through an inlet port, located in a larger base of the cone, and hence receives a swirl flow, which is maintained throughout the entire chamber length, all the way to an orifice in the narrow end of the truncated cone. In the resulting flow, peripheral velocity is increased when approaching the cylinder axis. Because of the centrifugal force in the swirl chamber, the pressure decreases towards its axis until it reaches an ambient pressure on the air core surface [26]. Therefore, it seems reasonable to perform experimental studies to determine the influence of the atomizer geometry on the spray angle value.

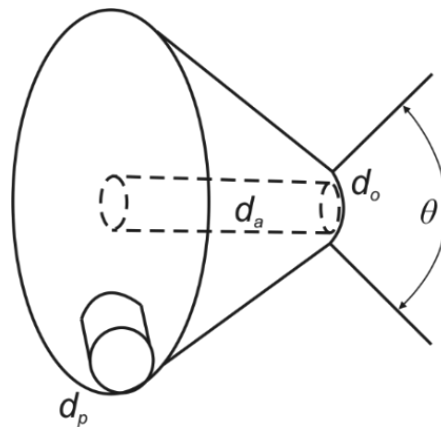


Figure 4. Schematic of the conical swirl chamber.

In Figures 5–7, the dependence of the spray angle on flow velocity is shown for non-Newtonian liquids (aqueous solutions of sodium carboxymethylcellulose at various concentrations). The increase in the concentration of the polymer in the solution resulted in a reduction of the spray angle for all tested liquids and for all analyzed atomizers, which is confirmed by the research of Broniarz-Press et al. [15]. In this case, the highest spray angles were obtained for a 0.1% aqueous solution of sodium carboxymethylcellulose, and the smallest spray angles were observed for a 0.4% aqueous Na-CMC solution.

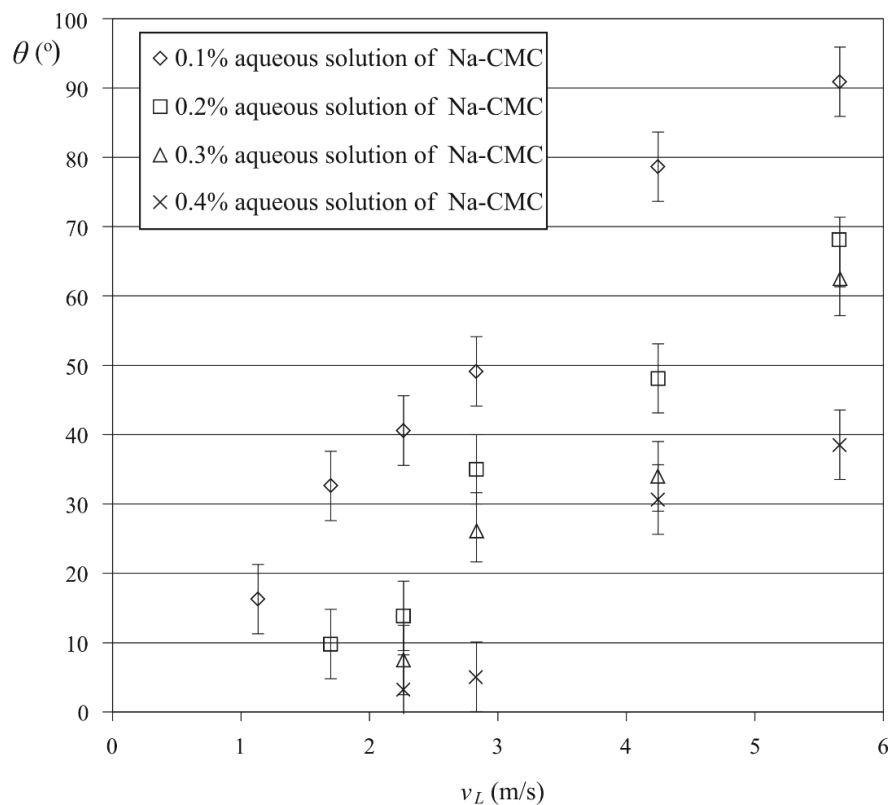


Figure 5. Dependence of the spray angle on the flow rate for the RSP1 atomizer.

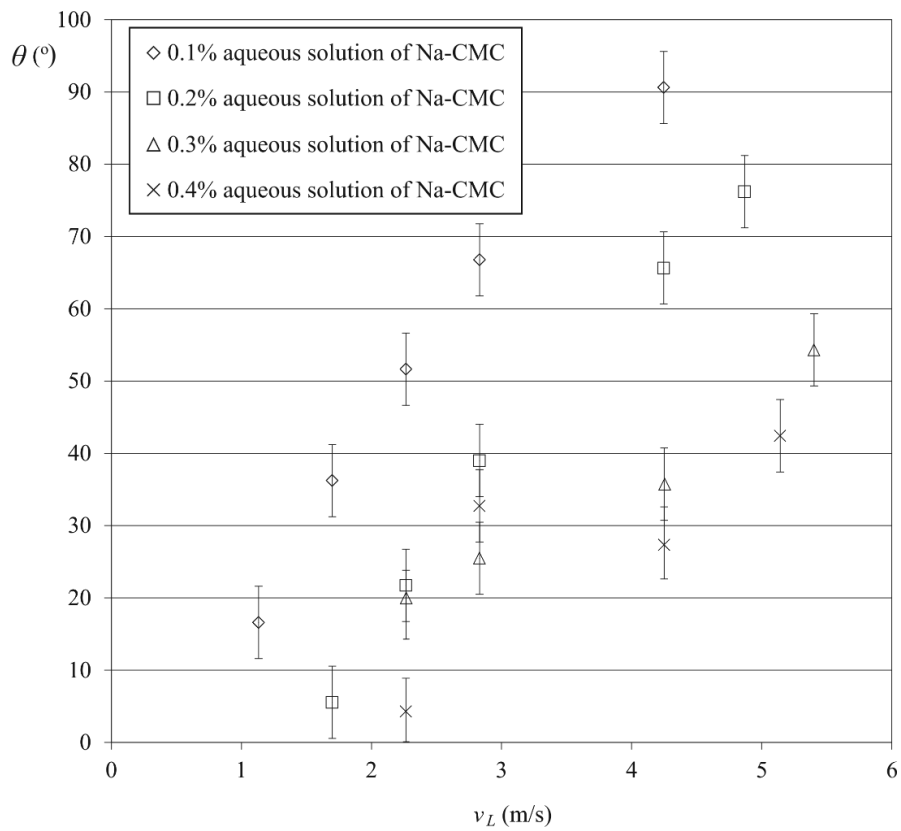


Figure 6. Dependence of the spray angle on the flow rate for the RSK1 atomizer.

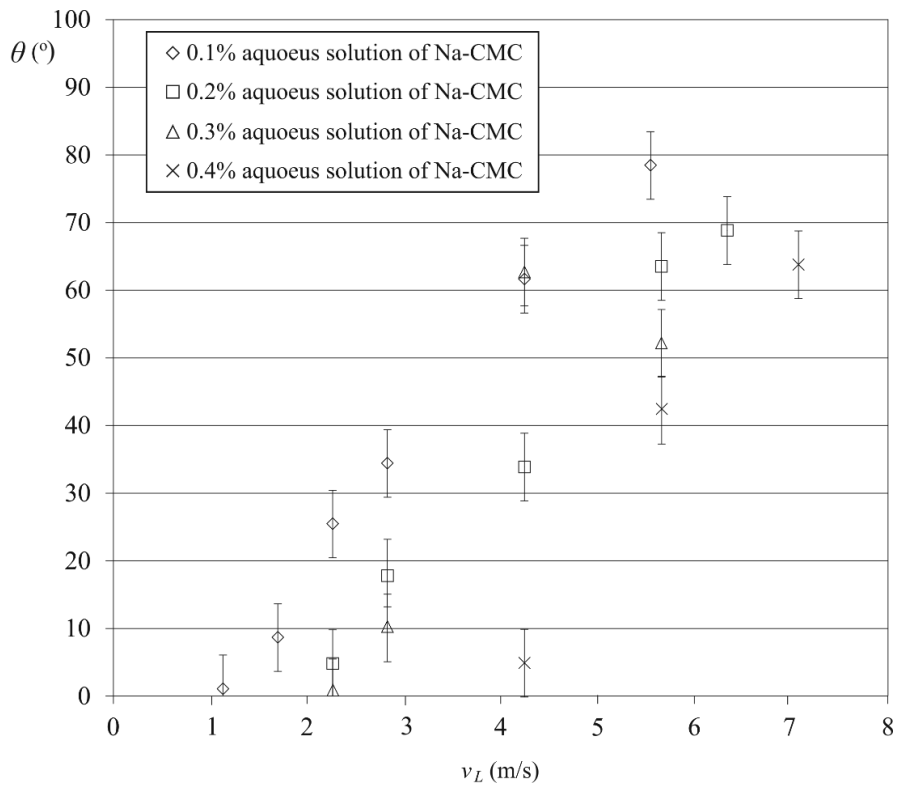
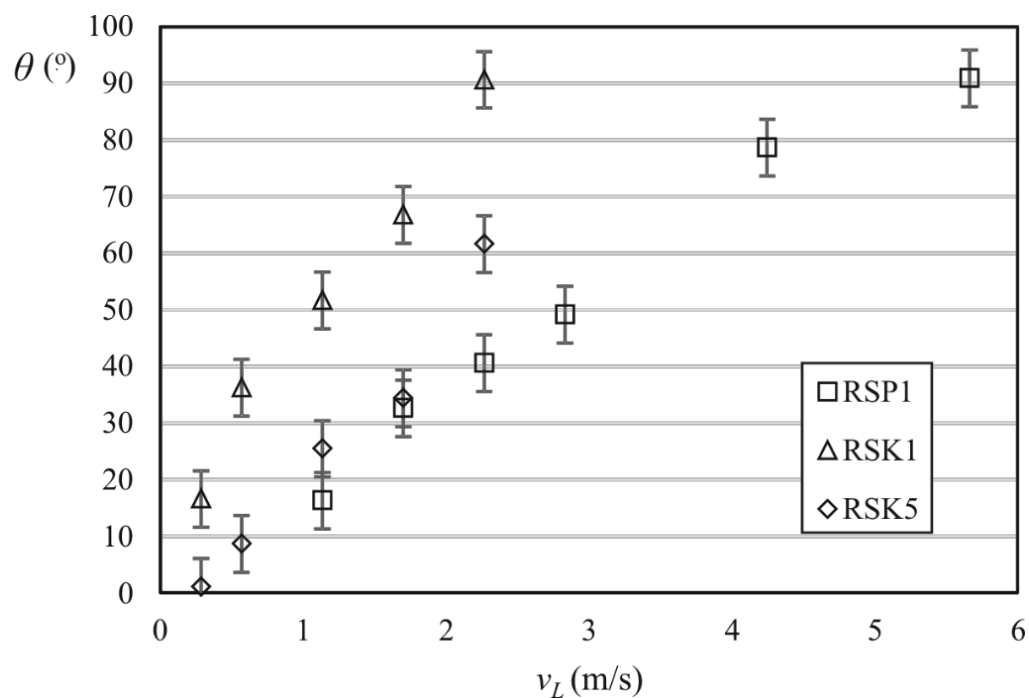


Figure 7. Dependence of the spray angle on the flow rate for the RSK5 atomizer.

Pressure-swirl atomizers are characterized by rotating motion of the liquid [27]. The swirl may be imposed by tangential feeding of the liquid. As this rotating flow exits the orifice, an annular liquid sheet is formed and breaks up on the droplets. The liquid flow rate depends on the pressure and the atomizer geometry, as well as the properties of the liquid. In Figures 5–7, we can observe the effect of the inclination angle of the inlet port. The use of an angular inlet port ( $\phi = 60^\circ$ , Figures 6 and 7), as compared to the inlet port perpendicular to the axis of the atomizer ( $\phi = 90^\circ$ , Figure 5), improved the spraying process—that is, the spray angles were wider. The literature review shows that the spray cone angle increases as the number of inlet ports is increased, which is in agreement with [28]. This observation can be attributed to the fact that more inlet ports tend to increase the azimuthal velocity inside the swirl chamber. A change in the inlet port angle  $\phi$  to an atomizer results in the reduction of angular momentum at the atomizer inlet port by the value of the function:  $\cos(90^\circ - \phi)$ .

Figure 8 shows an example of the dependence of the spray angle on the flow rate of a 0.1% sodium carboxymethylcellulose solution for various atomizer designs. We observed that the liquid inlet port at an angle in relation to the atomizer axis (RSK1) caused an increase in the spray angle as compared to the position perpendicular to the atomizer axis (RSP1). Larger spray angles were also achieved with a smaller swirl chamber diameter (RSK1) than with a larger diameter (RSK5). Figures 9 and 10 present the spray angle values for all tested atomizers. The highest spray angle was obtained for atomizers with  $D_S = 0.02$  m and an angular inlet port. The lowest spray angle was observed for atomizers with  $D_S = 0.04$  m. The influence of the height of the swirl chamber was not evident.



**Figure 8.** An example of the dependence of the spray angle on flow rate for a 0.1% aqueous solution of sodium carboxymethylcellulose for atomizers of various designs.

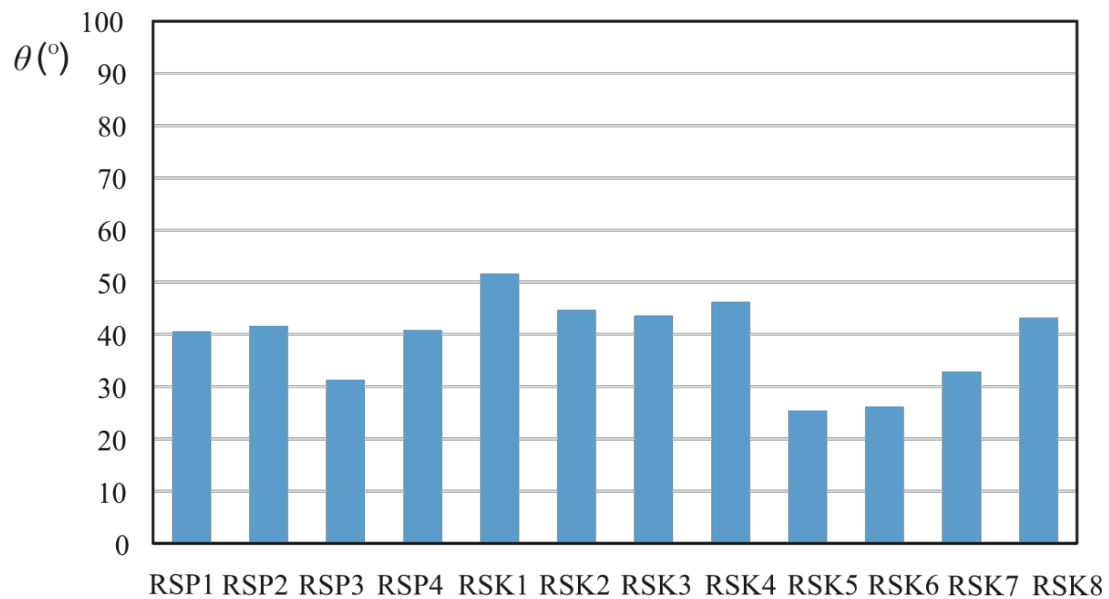


**Figure 9.** The spray angle values obtained by all tested atomizers for a 0.1% aqueous solution of Na-CMC for  $v_L = 2.26 \frac{m}{s}$ .

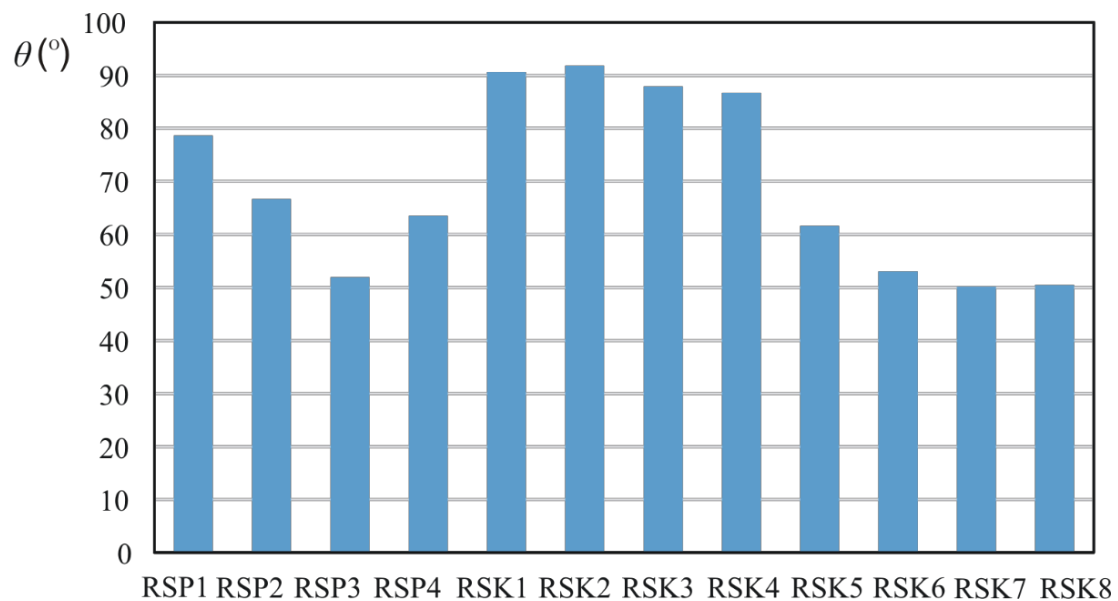


**Figure 10.** The spray angle values obtained by all tested atomizers for a 0.1% aqueous solution of Na-CMC for  $v_L = 4.25 \frac{m}{s}$ .

Figure 11 shows the relation between the spray angle tangent, the ratio of the orifice diameter to the swirl chamber height, and the liquid Reynolds number. The spray angle increased as the liquid Reynolds number increased. The ratio of the orifice diameter to the swirl chamber height did not significantly affect the spray angle tangent. The  $Re_L$  value decreases with increasing  $v_L$  and  $d_0$ , and a higher spray angle was observed. The  $Re_L$  value decreases with increasing liquid viscosity, and a lower spray angle was observed.

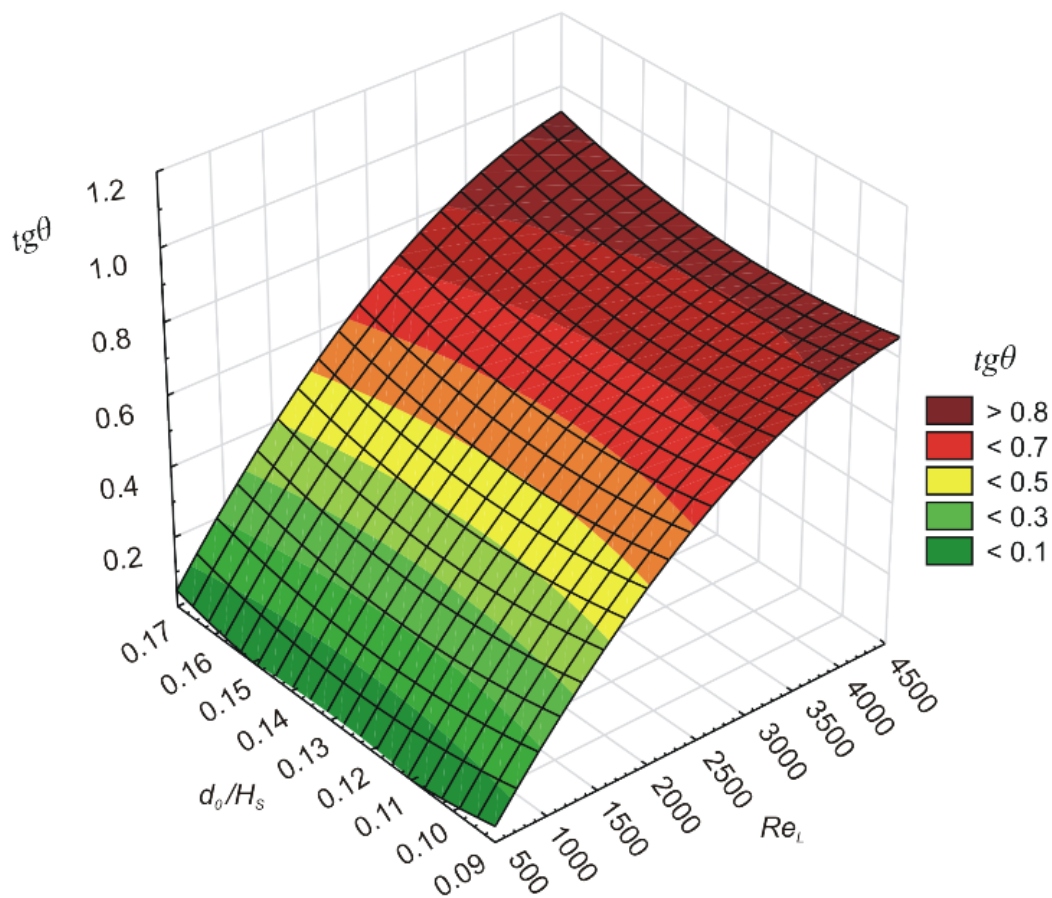


**Figure 11.** The relation between the spray angle tangent, the ratio of the orifice diameter to the swirl chamber height, and the liquid Reynolds number (angular inlet port of the liquid ( $\phi = 60^\circ$ )).

Based on the results obtained for atomizers with a conical swirl chamber and different inlet port inclinations, the following correlation equation describing the spray angle is proposed:

$$tg\theta = 4.2 \cdot 10^{-4} \cdot (\cos(90 - \varphi))^{-1.39} \cdot Re_L^{1.11} \cdot \left(\frac{d_0}{d_p}\right)^{0.05} \cdot \left(\frac{d_0}{D_S}\right)^{0.32} \cdot \left(\frac{d_0}{H_S}\right)^{0.42} \quad (5)$$

where  $Re_L$  is defined as:

$$Re_L = \frac{v_L^{2-n} \cdot d_0^n \cdot \rho_L}{8^{n-1} \cdot k} \quad (6)$$

This equation is correct for atomizers with a perpendicular inlet port and an inlet port positioned at an angle of  $60^\circ$  to the atomizer axis, in the Reynolds number range from 43 to 4000, with an orifice diameter of  $d_0 = 0.0025$  m, an inlet orifice diameter of  $d_p = 0.0025$  m, with an inlet port length from 0.00125 to 0.0025 m, a swirl chamber diameter ranging from 0.02 to 0.04 m, and a swirl chamber height between 0.015 and 0.025 m. The value of  $R$  equals 0.857. Figure 12 shows a comparison of the spray angle values obtained experimentally with the values calculated from Equation (5). The maximum deviation of the measurements was  $\pm 30\%$ .

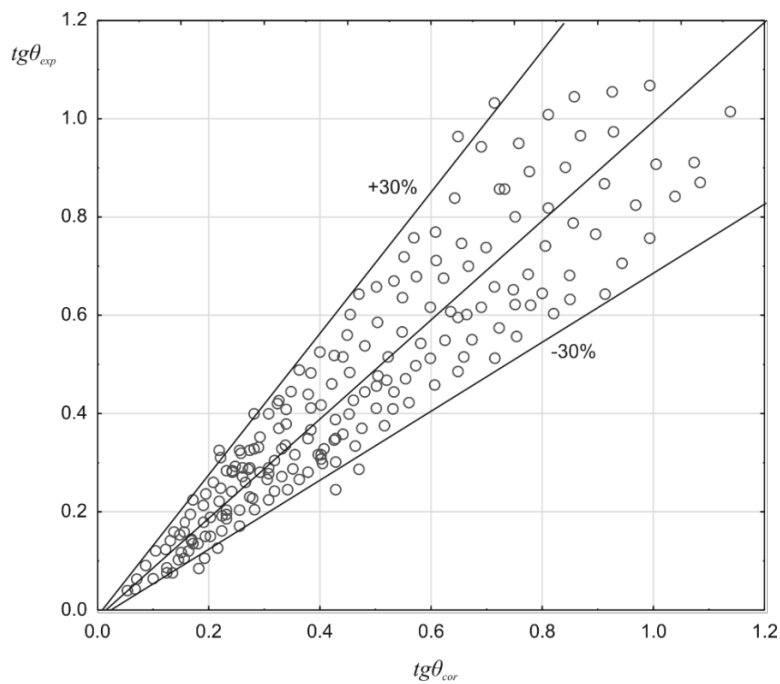


**Figure 12.** Comparison of the experimentally obtained spray angle tangent values with those calculated from Equation (5).

Figure 13 shows an example of the dependence of the spray half-angle tangent on the flow rate of a 0.1% Na-CMC solution for the RSP3 atomizer obtained on the basis of experimental data, calculations from the proposed correlation (Equation (5)), as well as Equation (1) proposed by Wójtowicz and Kotowski [18].

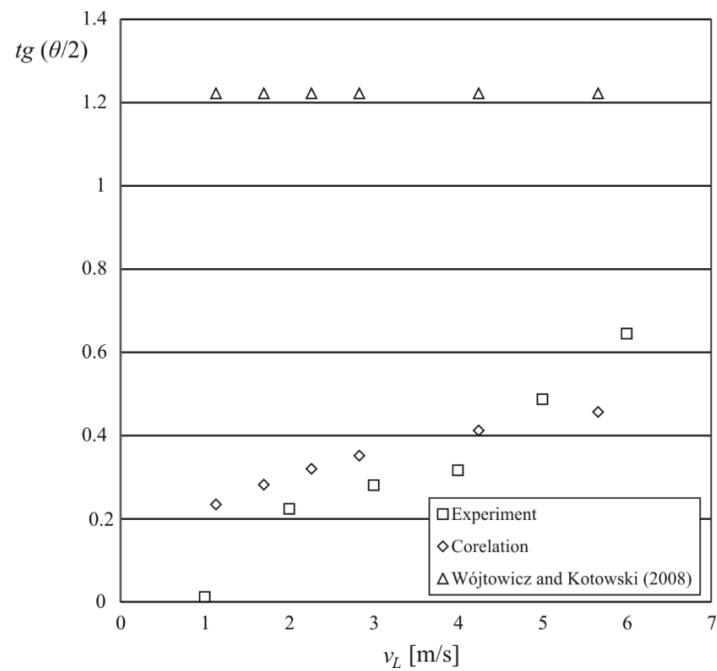


**Figure 13.** Comparison of the spray half-angle tangent of a 0.1% Na-CMC solution for the RSP3 atomizer obtained from experimental data with calculations from the proposed correlation (Equation (5)), and calculation from Equation (1), proposed by Wójtowicz and Kotowski [18].

The relation obtained on the basis of the equation of Wójtowicz and Kotowski [18] does not take into account the influence of operational parameters and liquid properties on the spray angle, and only considers the geometry of the equipment. Therefore, the discrepancies between the experimental data and the values of the tangent of the spray half-angle determined from this equation differ from the experimental data (i.e., they are much higher). The values determined on the basis of the proposed correlation (5) are similar to the experimental data. There are still no equations in the literature that account for all the factors influencing the spray angle value. Therefore, it seems reasonable to determine the dependence based on numerous experiments, taking the two-phase flow into account.

#### 4. Conclusions

Given the obtained results, we conclude that the spray breakdown manner and the spray angle are dependent on the viscosity of the liquid. The spray angle values decreased with increasing Na-CMC concentration (increasing viscosity). The spray angle was also significantly influenced by the atomizer geometry—especially the location of the inlet connector and the diameter of the swirl chamber. The use of an angular inlet port, as compared to a port perpendicular to the axis of the atomizer, improved the spraying process. Larger spray angles were also obtained when using an atomizer with a smaller swirl chamber diameter. Based on the research results, a correlation equation was proposed to determine the spray angle tangent depending on the Reynolds number and the atomizer geometry.

**Author Contributions:** Conceptualization, K.C., M.O.; Formal analysis, K.C., M.O.; Investigation, M.O., S.W.; Methodology, S.W.; Writing—original draft, K.C., M.O., S.W. All authors have read and agreed to the published version of the manuscript.

**Funding:** The scientific results presented in this article were obtained within the research project funded by the Ministry of Science and Higher Education of Poland.

**Conflicts of Interest:** The authors declare no conflict of interest.

#### References

1. Sobiech, Ł.; Grzanka, M.; Skrzypczak, G.; Idziak, R.; Włodarczak, S.; Ochowiak, M. Effect of adjuvants and pH adjuster on the efficacy of sulcotrione herbicide. *Agronomy* **2020**, *10*, 539. [[CrossRef](#)]
2. Ochowiak, M.; Broniarz-Press, L. Analysis of the breakup of aqueous polymer solution jet. *Chem. Eng. Equip.* **2007**, *4–5*, 91–93.
3. Som, S.K.; Mukherjee, S.G. Theoretical and experimental on the coefficient of discharge and spray cone angle of swirl spray atomizing nozzle. *Acta Mech.* **1980**, *32*, 79–102. [[CrossRef](#)]
4. Lee, E.J.; Oh, S.Y.; Kim, H.Y.; James, S.C.; Yoon, S.S. Measuring air core characteristics of a pressure-swirl atomizer via a transparent acrylic nozzle at various Reynolds numbers. *Exp. Therm. Fluid Sci.* **2010**, *34*, 1475–1483. [[CrossRef](#)]
5. Ochowiak, M.; Krupińska, A.; Włodarczak, S.; Matuszak, M.; Markowska, M.; Janczarek, M.; Szulc, T. The two-phase conical swirl atomizers: Spray characteristics. *Energies* **2020**, *13*, 3416. [[CrossRef](#)]
6. Lee, M.-Y.; Lee, G.-S.; Kim, C.-J.; Seo, J.-H.; Kim, K.-H. Macroscopic and microscopic spray characteristics of diesel and gasoline in a constant volume chamber. *Energies* **2018**, *11*, 2056. [[CrossRef](#)]
7. Fan, X.; Liu, C.; Mu, Y.; Wang, K.; Wang, Y.; Gang Xu, G. Experimental investigations of flow field and atomization field characteristics of pre-filming air-blast atomizers. *Energies* **2019**, *12*, 2800. [[CrossRef](#)]
8. Kim, K.; Lim, O. Investigation of the spray development process of gasoline-biodiesel blended fuel sprays in a constant volume chamber. *Energies* **2020**, *13*, 4819. [[CrossRef](#)]
9. Wang, X.; Huang, Z.; Kuti, O.A.; Zhang, W.; Nishida, K. Experimental and analytical study of biodiesel and diesel spray characteristics under ultra-high injection pressure. *Int. J. Heat Fluid Flow* **2010**, *4*, 659–666. [[CrossRef](#)]
10. Basak, A.; Patra, J.; Ganguly, R.; Datta, A. Effect of transesterification of vegetable oil on liquid flow number and spray cone angle for pressure and twin fluid atomizers. *Fuel* **2013**, *112*, 347–354. [[CrossRef](#)]
11. Yao, S.; Zhang, J.; Fang, T. Effect of viscosities on structure and instability of sprays from a swirl atomizer. *Exp. Therm. Fluid Sci.* **2012**, *39*, 158–166. [[CrossRef](#)]

12. Lee, S.; Park, S. Experimental study on spray break-up and atomization processes from GDI injector using high injection pressure up to 30 MPa. *Int. J. Heat Fluid Flow* **2014**, *45*, 14–22. [[CrossRef](#)]
13. Ochowiak, M.; Broniarz-Press, L.; Różańska, S.; Matuszak, M.; Włodarczak, S. Characteristics of spray angle for effervescent-swirl atomizers. *Chem. Eng. Process. Process Intensif.* **2015**, *98*, 52–59. [[CrossRef](#)]
14. Lefebvre, A.H. *Atomization and Sprays*; Hemisphere Publishing Corporation: New York, NY, USA, 1989.
15. Ballester, J.; Dopazo, C. Discharge coefficient and spray angle measurements for small pressure-swirl nozzles. *At. Sprays* **1994**, *4*, 351–367.
16. Zhang, T.; Dong, B.; Chen, X.; Qiu, Z.; Jiang, R.; Li, W. Spray characteristics of pressure-swirl nozzles at different nozzle. *Appl. Therm. Eng.* **2017**, *121*, 984–991. [[CrossRef](#)]
17. Rashad, M.; Yong, H.; Zekun, Z. Effect of geometric parameters on spray characteristics of pressure swirl atomizers. *Int. J. Hydrogen Energy* **2016**, *41*, 15790–15799. [[CrossRef](#)]
18. Durdina, L.; Jedelsky, J.; Jicha, M. Investigation and comparison of spray characteristics of pressure-swirl atomizers for a small-sized aircraft turbine engine. *Int. J. Heat Mass Transf.* **2014**, *78*, 892–900. [[CrossRef](#)]
19. Halder, M.R.; Dash, S.K.; Som, S.K. A numerical and experimental investigation on the coefficients of discharge and the spray cone angle of a solid cone swirl nozzle. *Exp. Therm. Fluid Sci.* **2004**, *28*, 297–305. [[CrossRef](#)]
20. Mun, R.P.; Byars, J.A.; Boger, D.V. Atomisation of dilute polymer solutions in agricultural spray nozzles. *J. Non-Newton. Fluid Mech.* **1999**, *83*, 163–178. [[CrossRef](#)]
21. Wójtowicz, P.; Kotowski, A. Badania modelowe stożkowych regulatorów hydrodynamicznych. *Ochrona Środowiska* **2008**, *3*, 37–44. (In Polish)
22. Ghannam, M.; Esmail, N. Flow behavior of enhanced oil recovery Alcoflood polymers. *J. Appl. Polym. Sci.* **2002**, *85*, 2896–2904. [[CrossRef](#)]
23. Zhang, L. Study on the Degradation and Stability for Flooding Polymers. Master's Thesis, University of Shandong, Shandong, China, 2011.
24. Chen, Y.Z.; Zhang, Z.; Chen, M.H.; Zhang, X.H.; Tian, Q.S.; Xing, L.M.; Ma, T. Analysis of the main factors affecting the viscosity of the solution of polymer. *Liaoning Chem. Ind.* **2004**, *33*, 258–260.
25. Durdina, L.; Jedelsky, J.; Jicha, M. Spray structure of a pressure-swirl atomizer for combustion applications. In *EPJ Web of Conferences*; EFM11—Experimental Fluid Mechanics 2011; EDP Sciences: Les Ulis, France, 2012; Volume 25, pp. 1–10.
26. Dafsari, R.A.; Vashahi, F.; Lee, J. Effect of swirl chamber length on the atomization characteristics of a pressure-swirl nozzle. *At. Sprays* **2017**, *27*, 859–874. [[CrossRef](#)]
27. Wimmer, E.; Brenn, G. Viscous flow through the swirl chamber of a pressure-swirl atomizer. *Int. J. Multiph. Flow* **2013**, *53*, 100–113. [[CrossRef](#)]
28. Mat Rashid, M.S.F.; Hamid, A.H.A.; Sheng, O.C.; Ghaffar, Z.A. Effect of Inlet Slot Number on the Spray Cone Angle and Discharge Coefficient of Swirl Atomizer. *Procedia Eng.* **2012**, *41*, 1781–1786. [[CrossRef](#)]

**Publisher's Note:** MDPI stays neutral with regard to jurisdictional claims in published maps and institutional affiliations.



© 2020 by the authors. Licensee MDPI, Basel, Switzerland. This article is an open access article distributed under the terms and conditions of the Creative Commons Attribution (CC BY) license (<http://creativecommons.org/licenses/by/4.0/>).